Study of ψ decays to the $\Xi^-\bar{\Xi}^+$ and $\Sigma(1385)^{\mp}\bar{\Sigma}(1385)^{\pm}$ final states

M. Ablikim[1], M. N. Achasov[9,e], X. C. Ai[1], O. Albayrak[5], M. Albrecht[4], D. J. Ambrose[44], A. Amoroso[49A,49C], F. F. An[1], Q. An[46,a], J. Z. Bai[1], R. Baldini Ferroli[20A], Y. Ban[31], D. W. Bennett[19], J. V. Bennett[5], M. Bertani[20A], D. Bettoni[21A], J. M. Bian[43], F. Bianchi[49A,49C], E. Boger[23,c], I. Boyko[23], R. A. Briere[5], H. Cai[51], X. Cai[1,a], O. Cakir[40A], A. Calcaterra[20A], G. F. Cao[1], S. A. Cetin[40B], J. F. Chang[1,a], G. Chelkov[23,c,d], G. Chen[1], H. S. Chen[1], H. Y. Chen[2], J. C. Chen[1], M. L. Chen[1,a], S. J. Chen[29], X. Chen[1,a], X. R. Chen[26], Y. B. Chen[1,a], H. P. Cheng[17], X. K. Chu[31], G. Cibinetto[21A], H. L. Dai[1,a], J. P. Dai[34], A. Dbeyssi[14], D. Dedovich[23], Z. Y. Deng[1], A. Denig[22], I. Denysenko[23], M. Destefanis[49A,49C], F. De Mori[49A,49C], Y. Ding[27], C. Dong[30], J. Dong[1,a], L. Y. Dong[1], M. Y. Dong[1,a], Z. L. Dou[29], S. X. Du[53], P. F. Duan[1], J. Z. Fan[39], J. Fang[1,a], S. S. Fang[1], X. Fang[46,a], Y. Fang[1], R. Farinelli[21A,21B], L. Fava[49B,49C], O. Fedorov[23], F. Feldbauer[22], G. Felici[20A], C. Q. Feng[46,a], E. Fioravanti[21A], M. Fritsch[14,22], C. D. Fu[1], Q. Gao[1], X. L. Gao[46,a], X. Y. Gao[2], Y. Gao[39], Z. Gao[46,a], I. Garzia[21A], K. Goetzen[10], L. Gong[30], W. X. Gong[1,a], W. Gradl[22], M. Greco[49A,49C], M. H. Gu[1,a], Y. T. Gu[12], Y. H. Guan[1], A. Q. Guo[1], L. B. Guo[28], Y. Guo[1], Y. P. Guo[22], Z. Haddadi[25], A. Hafner[22], S. Han[51], X. Q. Hao[15], F. A. Harris[42], K. L. He[1], T. Held[4], Y. K. Heng[1,a], Z. L. Hou[1], C. Hu[28], H. M. Hu[1], J. F. Hu[49A,49C], T. Hu[1,a], Y. Hu[1], G. S. Huang[46,a], J. S. Huang[15], X. T. Huang[33], Y. Huang[29], T. Hussain[48], Q. Ji[1], Q. P. Ji[30], X. B. Ji[1], X. L. Ji[1,a], L. W. Jiang[51], X. S. Jiang[1,a], X. Y. Jiang[30], J. B. Jiao[33], Z. Jiao[17], D. P. Jin[1,a], S. Jin[1], T. Johansson[50], A. Julin[43], N. Kalantar-Nayestanaki[25], X. L. Kang[1], X. S. Kang[30], M. Kavatsyuk[25], B. C. Ke[5], P. Kiese[22], R. Kliemt[14], B. Kloss[22], O. B. Kolcu[40B,h], B. Kopf[4], M. Kornicer[42], A. Kupsc[50], W. Kühn[24], J. S. Lange[24], M. Lara[19], P. Larin[14], C. Leng[49C], C. Li[50], Cheng Li[46,a], D. M. Li[53], F. Li[1,a], F. Y. Li[31], G. Li[1], H. B. Li[1], J. C. Li[1], Jin Li[32], K. Li[33], K. Li[13], Lei Li[3], P. R. Li[41], Q. Y. Li[33], T. Li[33], W. D. Li[1], W. G. Li[1], X. L. Li[33], X. N. Li[1,a], X. Q. Li[30], Z. B. Li[38], H. Liang[46,a], Y. F. Liang[36], Y. T. Liang[24], G. R. Liao[11], D. X. Lin[14], B. J. Liu[1], C. X. Liu[1], D. Liu[46,a], F. H. Liu[35], Fang Liu[1], Feng Liu[6], H. B. Liu[12], H. H. Liu[16], H. H. Liu[1], H. M. Liu[1], J. Liu[1], J. B. Liu[46,a], J. P. Liu[51], J. Y. Liu[1], K. Liu[39], K. Y. Liu[27], L. D. Liu[31], P. L. Liu[1,a], Q. Liu[41], S. B. Liu[46,a], X. Liu[26], Y. B. Liu[30], Z. A. Liu[1,a], Zhiqing Liu[22], H. Loehner[25], X. C. Lou[1,a,g], H. J. Lu[17], J. G. Lu[1,a], Y. Lu[1], Y. P. Lu[1,a], C. L. Luo[28], M. X. Luo[52], T. Luo[42], X. L. Luo[1,a], X. R. Lyu[41], F. C. Ma[27], H. L. Ma[1], L. L. Ma[33], Q. M. Ma[1], T. Ma[1], X. N. Ma[30], X. Y. Ma[1,a], Y. M. Ma[33], F. E. Maas[14], M. Maggiora[49A,49C], Y. J. Mao[31], Z. P. Mao[1], S. Marcello[49A,49C], J. G. Messchendorp[25], J. Min[1,a], R. E. Mitchell[19], X. H. Mo[1,a], Y. J. Mo[6], C. Morales Morales[14], N. Yu. Muchnoi[9,e], H. Muramatsu[43], Y. Nefedov[23], F. Nerling[14], I. B. Nikolaev[9,e], Z. Ning[1,a], S. Nisar[8], S. L. Niu[1,a], X. Y. Niu[1], S. L. Olsen[32], Q. Ouyang[1,a], S. Pacetti[20B], Y. Pan[46,a], P. Patteri[20A], M. Pelizaeus[4], H. P. Peng[46,a], K. Peters[10], J. Pettersson[50], J. L. Ping[28], R. G. Ping[1], R. Poling[43], V. Prasad[1], H. R. Qi[2], M. Qi[29], S. Qian[1,a], C. F. Qiao[41], L. Q. Qin[33], N. Qin[51], X. S. Qin[1], Z. H. Qin[1,a], J. F. Qiu[1], K. H. Rashid[48], C. F. Redmer[22], M. Ripka[22], G. Rong[1], Ch. Rosner[14], X. D. Ruan[12], V. Santoro[21A], A. Sarantsev[23,f], M. Savrié[21B], K. Schoenning[50], S. Schumann[22], W. Shan[31], M. Shao[46,a], C. P. Shen[2], P. X. Shen[30], X. Y. Shen[1], H. Y. Sheng[1], W. M. Song[1], X. Y. Song[1], S. Sosio[49A,49C], S. Spataro[49A,49C], G. X. Sun[1], J. F. Sun[15], S. S. Sun[1], Y. J. Sun[46,a], Y. Z. Sun[1], Z. J. Sun[1,a], Z. T. Sun[19], C. J. Tang[36], X. Tang[1], I. Tapan[40C], E. H. Thorndike[44], M. Tiemens[25], M. Ullrich[24], I. Uman[40D], G. S. Varner[42], B. Wang[30], B. L. Wang[41], D. Wang[31], D. Y. Wang[31], K. Wang[1,a], L. L. Wang[1], L. S. Wang[1], M. Wang[33], P. Wang[1], P. L. Wang[1], S. G. Wang[31], W. Wang[1,a], W. P. Wang[46,a], X. F. Wang[39], Y. D. Wang[14], Y. F. Wang[1,a], Y. Q. Wang[22], Z. Wang[1,a], Z. G. Wang[1,a], Z. H. Wang[46,a], Z. Y. Wang[1], T. Weber[22], D. H. Wei[11], J. B. Wei[31], P. Weidenkaff[22], S. P. Wen[1], U. Wiedner[4], M. Wolke[50], L. H. Wu[1], Z. Wu[1,a], L. Xia[46,a], L. G. Xia[39], Y. Xia[18], D. Xiao[1], H. Xiao[47], Z. J. Xiao[28], Y. G. Xie[1,a], Q. L. Xiu[1,a], G. F. Xu[1], L. Xu[1], Q. J. Xu[13], Q. N. Xu[41], X. P. Xu[37], L. Yan[49A,49C], W. B. Yan[46,a], W. C. Yan[46,a], Y. H. Yan[18], H. J. Yang[34], H. X. Yang[1], L. Yang[51], Y. X. Yang[11], M. Ye[1,a], M. H. Ye[7], J. H. Yin[1], B. X. Yu[1,a], C. X. Yu[30], J. S. Yu[26], C. Z. Yuan[1], W. L. Yuan[29], Y. Yuan[1], A. Yuncu[40B,b], A. A. Zafar[48], A. Zallo[20A], Y. Zeng[18], Z. Zeng[46,a], B. X. Zhang[1], B. Y. Zhang[1,a], C. Zhang[29], C. C. Zhang[1], D. H. Zhang[1], H. H. Zhang[38], H. Y. Zhang[1,a], J. J. Zhang[1], J. L. Zhang[1], J. Q. Zhang[1], J. W. Zhang[1,a], J. Y. Zhang[1], J. Z. Zhang[1], K. Zhang[1], L. Zhang[1], X. Y. Zhang[33], Y. Zhang[1], Y. H. Zhang[1,a], Y. N. Zhang[41], Y. T. Zhang[46,a], Yu Zhang[41], Z. H. Zhang[6], Z. P. Zhang[46], Z. Y. Zhang[51], G. Zhao[1], J. W. Zhao[1,a], J. Y. Zhao[1], J. Z. Zhao[1,a], Lei Zhao[46,a], Ling Zhao[1], M. G. Zhao[30], Q. Zhao[1], Q. W. Zhao[1], S. J. Zhao[53], T. C. Zhao[1], Y. B. Zhao[1,a], Z. G. Zhao[46,a], A. Zhemchugov[23,c], B. Zheng[47], J. P. Zheng[1,a], W. J. Zheng[33], Y. H. Zheng[41], B. Zhong[28], L. Zhou[1,a], X. Zhou[51], X. K. Zhou[46,a], X. R. Zhou[46,a], X. Y. Zhou[1], K. Zhu[1], K. J. Zhu[1,a], S. Zhu[1], S. H. Zhu[45], X. L. Zhu[39], Y. C. Zhu[46,a], Y. S. Zhu[1], Z. A. Zhu[1], J. Zhuang[1,a], L. Zotti[49A,49C], B. S. Zou[1], J. H. Zou[1]

(BESIII Collaboration)

[1] *Institute of High Energy Physics, Beijing 100049, People's Republic of China*
[2] *Beihang University, Beijing 100191, People's Republic of China*
[3] *Beijing Institute of Petrochemical Technology, Beijing 102617, People's Republic of China*
[4] *Bochum Ruhr-University, D-44780 Bochum, Germany*

[5] *Carnegie Mellon University, Pittsburgh, Pennsylvania 15213, USA*

[6] *Central China Normal University, Wuhan 430079, People's Republic of China*

[7] *China Center of Advanced Science and Technology, Beijing 100190, People's Republic of China*

[8] *COMSATS Institute of Information Technology, Lahore, Defence Road, Off Raiwind Road, 54000 Lahore, Pakistan*

[9] *G.I. Budker Institute of Nuclear Physics SB RAS (BINP), Novosibirsk 630090, Russia*

[10] *GSI Helmholtzcentre for Heavy Ion Research GmbH, D-64291 Darmstadt, Germany*

[11] *Guangxi Normal University, Guilin 541004, People's Republic of China*

[12] *GuangXi University, Nanning 530004, People's Republic of China*

[13] *Hangzhou Normal University, Hangzhou 310036, People's Republic of China*

[14] *Helmholtz Institute Mainz, Johann-Joachim-Becher-Weg 45, D-55099 Mainz, Germany*

[15] *Henan Normal University, Xinxiang 453007, People's Republic of China*

[16] *Henan University of Science and Technology, Luoyang 471003, People's Republic of China*

[17] *Huangshan College, Huangshan 245000, People's Republic of China*

[18] *Hunan University, Changsha 410082, People's Republic of China*

[19] *Indiana University, Bloomington, Indiana 47405, USA*

[20] *(A)INFN Laboratori Nazionali di Frascati, I-00044, Frascati, Italy; (B)INFN and University of Perugia, I-06100, Perugia, Italy*

[21] *(A)INFN Sezione di Ferrara, I-44122, Ferrara, Italy; (B)University of Ferrara, I-44122, Ferrara, Italy*

[22] *Johannes Gutenberg University of Mainz, Johann-Joachim-Becher-Weg 45, D-55099 Mainz, Germany*

[23] *Joint Institute for Nuclear Research, 141980 Dubna, Moscow region, Russia*

[24] *Justus-Liebig-Universitaet Giessen, II. Physikalisches Institut, Heinrich-Buff-Ring 16, D-35392 Giessen, Germany*

[25] *KVI-CART, University of Groningen, NL-9747 AA Groningen, The Netherlands*

[26] *Lanzhou University, Lanzhou 730000, People's Republic of China*

[27] *Liaoning University, Shenyang 110036, People's Republic of China*

[28] *Nanjing Normal University, Nanjing 210023, People's Republic of China*

[29] *Nanjing University, Nanjing 210093, People's Republic of China*

[30] *Nankai University, Tianjin 300071, People's Republic of China*

[31] *Peking University, Beijing 100871, People's Republic of China*

[32] *Seoul National University, Seoul, 151-747 Korea*

[33] *Shandong University, Jinan 250100, People's Republic of China*

[34] *Shanghai Jiao Tong University, Shanghai 200240, People's Republic of China*

[35] *Shanxi University, Taiyuan 030006, People's Republic of China*

[36] *Sichuan University, Chengdu 610064, People's Republic of China*

[37] *Soochow University, Suzhou 215006, People's Republic of China*

[38] *Sun Yat-Sen University, Guangzhou 510275, People's Republic of China*

[39] *Tsinghua University, Beijing 100084, People's Republic of China*

[40] *(A)Ankara University, 06100 Tandogan, Ankara, Turkey; (B)Istanbul Bilgi University, 34060 Eyup, Istanbul, Turkey; (C)Uludag University, 16059 Bursa, Turkey; (D)Near East University, Nicosia, North Cyprus, Mersin 10, Turkey*

[41] *University of Chinese Academy of Sciences, Beijing 100049, People's Republic of China*

[42] *University of Hawaii, Honolulu, Hawaii 96822, USA*

[43] *University of Minnesota, Minneapolis, Minnesota 55455, USA*

[44] *University of Rochester, Rochester, New York 14627, USA*

[45] *University of Science and Technology Liaoning, Anshan 114051, People's Republic of China*

[46] *University of Science and Technology of China, Hefei 230026, People's Republic of China*

[47] *University of South China, Hengyang 421001, People's Republic of China*

[48] *University of the Punjab, Lahore-54590, Pakistan*

[49] *(A)University of Turin, I-10125, Turin, Italy; (B)University of Eastern Piedmont, I-15121, Alessandria, Italy; (C)INFN, I-10125, Turin, Italy*

[50] *Uppsala University, Box 516, SE-75120 Uppsala, Sweden*

[51] *Wuhan University, Wuhan 430072, People's Republic of China*

[52] *Zhejiang University, Hangzhou 310027, People's Republic of China*

[53] *Zhengzhou University, Zhengzhou 450001, People's Republic of China*

[a] *Also at State Key Laboratory of Particle Detection and Electronics, Beijing 100049, Hefei 230026, People's Republic of China*

[b] *Also at Bogazici University, 34342 Istanbul, Turkey*
[c] *Also at the Moscow Institute of Physics and Technology, Moscow 141700, Russia*
[d] *Also at the Functional Electronics Laboratory, Tomsk State University, Tomsk, 634050, Russia*
[e] *Also at the Novosibirsk State University, Novosibirsk, 630090, Russia*
[f] *Also at the NRC "Kurchatov Institute", PNPI, 188300, Gatchina, Russia*
[g] *Also at University of Texas at Dallas, Richardson, Texas 75083, USA*
[h] *Also at Istanbul Arel University, 34295 Istanbul, Turkey*

Abstract

We study the decays of the charmonium resonances J/ψ and $\psi(3686)$ to the final states $\Xi^-\bar{\Xi}^+$, $\Sigma(1385)^\mp\bar{\Sigma}(1385)^\pm$ based on a single baryon tag method using data samples of $(223.7 \pm 1.4) \times 10^6$ J/ψ and $(106.4 \pm 0.9) \times 10^6$ $\psi(3686)$ events collected with the BESIII detector at the BEPCII collider. The decay $\psi(3686) \to \Sigma(1385)^\mp\bar{\Sigma}(1385)^\pm$ is observed for the first time, and the measurements of the other processes, including the branching fractions and angular distributions, are in good agreement with, and much more precise than, the previously published results. Additionally, the ratios $\frac{\mathcal{B}(\psi(3686)\to\Xi^-\bar{\Xi}^+)}{\mathcal{B}(J/\psi\to\Xi^-\bar{\Xi}^+)}$, $\frac{\mathcal{B}(\psi(3686)\to\Sigma(1385)^-\bar{\Sigma}(1385)^+)}{\mathcal{B}(J/\psi\to\Sigma(1385)^-\bar{\Sigma}(1385)^+)}$ and $\frac{\mathcal{B}(\psi(3686)\to\Sigma(1385)^+\bar{\Sigma}(1385)^-)}{\mathcal{B}(J/\psi\to\Sigma(1385)^+\bar{\Sigma}(1385)^-)}$ are determined.

PACS numbers: 12.38.Qk, 13.25.Gv, 23.20.En

I. INTRODUCTION

The study of ψ [in the following, ψ denotes both charmonium resonances J/ψ and $\psi(3686)$] production in e^+e^- annihilation and the subsequent two-body hadronic decays of the ψ, such as baryon-antibaryon decays, provide a unique opportunity to test quantum chromodynamics (QCD) in the perturbative energy regime and to study the baryonic properties [1]. These decays are expected to proceed via the annihilation of $c\bar{c}$ into three gluons or a virtual photon. This model also leads to the prediction that the ratio of the branching fractions of ψ decays to a specific final state should follow the so-called "12% rule" [2]

$$\frac{\mathcal{B}(\psi(3686) \to \text{hadrons})}{\mathcal{B}(J/\psi \to \text{hadrons})} \approx \frac{\mathcal{B}(\psi(3686) \to e^+e^-)}{\mathcal{B}(J/\psi \to e^+e^-)} \approx 12\%, \tag{1}$$

where the branching fractions probe the ratio of the wave functions at their origins for the vector ground state J/ψ and its first radial excitation $\psi(3686)$. This rule was first observed to be violated in the process $\psi \to \rho\pi$, which is known as the "$\rho\pi$ puzzle," and was subsequently further tested in a wide variety of experimental measurements [3]. Recently, a review of the theoretical and experimental results [4] concluded that the current theoretical explanations are unsatisfactory, especially for the baryon pair decays of ψ mesons. Therefore, more experimental measurements on baryon-antibaryon $(B\bar{B})$ pair final states, e.g. $p\bar{p}, \Lambda\bar{\Lambda}, \Sigma\bar{\Sigma}, \Xi\bar{\Xi}, \Sigma(1385)\bar{\Sigma}(1385)$, in the decays of ψ are desirable. To date, the branching fractions of the decays $\psi \to \Xi^-\bar{\Xi}^+$ and $J/\psi \to \Sigma(1385)^\mp\bar{\Sigma}(1385)^\pm$ were previously measured with a low precision [5–9], and the decay $\psi(3686) \to \Sigma(1385)^\mp\bar{\Sigma}(1385)^\pm$ has not yet been observed.

By using hadron helicity conservation, the angular distribution for the process $e^+e^- \to \psi \to B\bar{B}$ can be expressed as

$$\frac{dN}{d(\cos\theta)} \propto 1 + \alpha\cos^2\theta, \tag{2}$$

where θ is the angle between the baryon and the positron-beam direction in the e^+e^- center-of-mass (CM) system and α is a constant. Various theoretical calculations based on first-order QCD have made predictions for the value of α. In the prediction of Claudson *et al.* [10], the baryon mass is taken into account as a whole, while the constituent quarks inside the baryon are considered as massless when computing the decay amplitude. The prediction by Carimalo [11] takes the mass effects at the quark level into account. Experimental efforts are useful to measure α in order to test the hadron helicity conservation rule and study the validity of the various theoretical approaches. In the previous experiments, the angular distributions are measured with a few decays, such as $\psi(3686) \to p\bar{p}$ [12] and $J/\psi \to B\bar{B}$ [$p\bar{p}, \Lambda\bar{\Lambda}, \Sigma^0\bar{\Sigma}^0, \Xi^-\bar{\Xi}^+, \Sigma(1385)\bar{\Sigma}(1385)$] [8, 13–15]. Among them, the angular distributions for the $J/\psi \to \Xi^-\bar{\Xi}^+, \Sigma(1385)^\mp\bar{\Sigma}(1385)^\pm$ decays are determined with a low precision, while for the decays $\psi(3686) \to \Xi^-\bar{\Xi}^+$, $\Sigma(1385)^\mp\bar{\Sigma}(1385)^\pm$ have not yet been measured.

In this paper, we report the most precise measurements of the branching fractions and angular distributions for the decays $\psi \to \Xi^-\bar{\Xi}^+, \Sigma(1385)^\mp\bar{\Sigma}(1385)^\pm$ based on $(223.7 \pm 1.4) \times 10^6$ J/ψ [17] and $(106.4 \pm 0.9) \times 10^6$ $\psi(3686)$ [18] events collected with the BESIII detector at BEPCII.

II. BESIII DETECTOR AND MONTE CARLO SIMULATION

BEPCII is a double-ring e^+e^- collider that has reached a peak luminosity of about 8.5×10^{32} $\text{cm}^{-2}\text{s}^{-1}$ at a CM energy of 3.773 GeV. The cylindrical core of the BESIII detector consists of a helium-based main drift chamber (MDC), a plastic scintillator time-of-flight (TOF) system, and a CsI(Tl) electromagnetic calorimeter (EMC), which are all enclosed in a superconducting solenoidal magnet with a field strength of 1.0 T. The solenoid is supported by an octagonal flux-return yoke with resistive plate counter modules interleaved with steel as muon identifier. The acceptance for charged particles and photons is 93% over 4π stereo angle, and the

charged-particle momentum resolution at 1 GeV/c is 0.5%, the photon energy resolution at 1.0 GeV is 2.5% (5%) in the barrel (end caps). More details about the apparatus can be found in Ref. [19].

The response of the BESIII detector is modeled with Monte Carlo (MC) simulations using a framework based on GEANT4 [20, 21]. The production of ψ resonances is simulated with the KKMC generator [22], while the subsequent decays are processed via EVTGEN [23] according to the branching fractions provided by the Particle Data Group (PDG) [3], and the remaining unmeasured decay modes are generated with LUNDCHARM [24]. To determine the detection efficiencies for $\psi \to \Xi^- \bar{\Xi}^+$, $\Sigma(1385)^\mp \bar{\Sigma}(1385)^\pm$, one million MC events are generated for each mode, corresponding to samples about $20 \sim 50$ times larger than expected in data. The events are generated for each channel with our measured angular distribution parameter, which we will introduce in detail later; the Ξ and $\Sigma(1385)$ decays in the signal modes are simulated inclusively according to the corresponding branching fractions taken from PDG [3].

III. EVENT SELECTION

The selection of $\psi \to \Xi^- \bar{\Xi}^+$, $\Sigma(1385)^\mp \bar{\Sigma}(1385)^\pm$ events via a full reconstruction of both $\Xi^-(\Sigma(1385)^\mp)$ and $\bar{\Xi}^+(\bar{\Sigma}(1385)^\pm)$ baryons suffers from low reconstruction efficiency. To achieve a higher efficiency, a single baryon Ξ^- $(\Sigma(1385)^\mp)$ tag technique, which does not include the antibaryon mode tag, is employed to select the signal events $\psi \to \Xi^- \bar{\Xi}^+(\Sigma(1385)^\mp \bar{\Sigma}(1385)^\pm)$, where only the $\Xi^-(\Sigma(1385)^\mp)$ is reconstructed in its decay to $\pi^\mp \Lambda$ with the subsequent decay $\Lambda \to p\pi^-$. Thus, we require that the events contain at least one positively charged and two negatively charged tracks for the $\Xi^- \bar{\Xi}^+(\Sigma(1385)^- \bar{\Sigma}(1385)^+)$ channel and two positively charged and one negatively charged track for the $\Sigma(1385)^+ \bar{\Sigma}(1385)^-$ channel. Only tracks that are reconstructed in the MDC with good helix fits and within the angular coverage of the MDC ($|\cos\theta| < 0.93$, where θ is the polar angle with respect to the e^+ beam direction) are considered. Information from the specific energy loss measured in MDC (dE/dx) and from TOF are combined to form particle identification (PID) confidence levels for the hypotheses of a pion, kaon, and proton, respectively. Each track is assigned to the particle type that corresponds to the hypothesis with the highest confidence level. Events with at least two charged pions ($\pi^- \pi^\mp$) and at least one proton (p) are kept for further analysis.

In order to reconstruct Λ baryons, a vertex fit is applied to all $p\pi^-$ combinations; the ones characterized by $\chi^2 < 500$ are selected. The invariant mass of the $p\pi^-$ pair is required to be within 6 MeV/c^2 of the nominal Λ mass. Subsequently, candidates for Ξ^- and $\Sigma(1385)^\mp$ baryons are built by combining all reconstructed Λ with another $\pi^\mp$. The combination with the minimum $|M_{\pi^\mp\Lambda} - M_{\Xi^-/\Sigma(1385)^\mp}|$ is selected, where

$M_{\Xi^-/\Sigma(1385)^\mp}$ is the nominal mass of Ξ^- or $\Sigma(1385)^\mp$ from PDG [3].

The partner of $\bar{\Xi}^+$ or $\bar{\Sigma}(1385)^\pm$ is extracted from the mass recoiling against the selected $\pi^\mp \Lambda$ system,

$$M_{\pi^\mp\Lambda}^{\rm recoil} = \sqrt{(E_{CM} - E_{\pi^\mp\Lambda})^2 - \vec{p}_{\pi^\mp\Lambda}^{\,2}}, \qquad (3)$$

where $E_{\pi^\mp\Lambda}$ and $\vec{p}_{\pi^\mp\Lambda}$ are the energy and the momentum of the selected $\pi^\mp \Lambda$ system, respectively, and E_{CM} is the e^+e^- CM energy. Figure 1 shows the scatter plots of $M_{\pi^\mp\Lambda}$ versus $M_{\pi^\mp\Lambda}^{\rm recoil}$ for the J/ψ and $\psi(3686)$ data samples. Clear accumulations of events are found for the signals of $\psi \to \Xi^- \bar{\Xi}^+$ ($\Sigma(1385)^\mp \bar{\Sigma}(1385)^\pm$) decays. To determine the signal yields, the mass of $\pi^\mp \Lambda$ is required to be in the interval $[1.312, 1.332]$ GeV/c^2 for $J/\psi \to \Xi^- \bar{\Xi}^+$, and $[1.308, 1.338]$ GeV/c^2 for $\psi(3686) \to \Xi^- \bar{\Xi}^+$, respectively, while we require $|M_{\pi^\mp\Lambda} - M_{\Sigma(1385)^\mp}| < 0.035$ GeV/c^2 for $\psi \to \Sigma(1385)^\mp \bar{\Sigma}(1385)^\pm$. For the decay $\psi(3686) \to \Xi^- \bar{\Xi}^+$ ($\Sigma(1385)^- \bar{\Sigma}(1385)^+$), a further requirement of $|M_{\pi^+\pi^-}^{\rm recoil} - M_{J/\psi}| > 0.005$ GeV/c^2 is applied to suppress the background $\psi(3686) \to \pi^+\pi^- J/\psi$, where the $M_{\pi^+\pi^-}^{\rm recoil}$ is the recoil mass of all $\pi^+\pi^-$ combination, and $M_{J/\psi}$ is the nominal mass of J/ψ according to the PDG [3].

IV. BACKGROUND STUDY

Data collected at center-of-mass energies of 3.08 GeV (300 nb^{-1} [17]) and 3.65 GeV (44 pb^{-1} [18]) are used to estimate the contributions from the continuum processes $e^+e^- \to \Xi^- \bar{\Xi}^+, \Sigma(1385)^\mp \bar{\Sigma}(1385)^\pm$. After applying the same event selection criteria, only a few events survive, which do not form any obvious peaking structures around the $\bar{\Xi}^+$ or $\bar{\Sigma}(1835)^\pm$ signal regions in the corresponding $M_{\pi^\mp\Lambda}^{\rm recoil}$ distribution. The scale factor between the data at $\psi(3686)$ peak and that at 3.65 GeV is 3.677, taking into account the luminosity and CM energy dependence of the cross section. This implies that the backgrounds from continuum processes are negligible.

The contamination from other background sources is studied by using MC simulated samples of generic ψ decays that contain the same number of events as data. After applying the same event selection criteria, it is found that the channels $J/\psi \to \gamma\eta_c$ with $\eta_c \to \Xi^- \bar{\Xi}^+$, $J/\psi \to \pi^- \Lambda\Sigma(1385)^+$ (the branching fraction is preliminarily determined with the data based on an iterative method), and $J/\psi \to \Sigma(1385)^- \bar{\Sigma}(1385)^+$ are potential peaking backgrounds for $J/\psi \to \Xi^- \bar{\Xi}^+$. According to MC simulations of these backgrounds, their yields are expected to be negligible after normalization to the total number of J/ψ events. For the $J/\psi \to \Sigma(1385)^\mp \bar{\Sigma}(1385)^\pm$ decay, backgrounds are found to be $J/\psi \to \pi^\mp \Lambda\bar{\Sigma}(1385)^\pm$, $J/\psi \to \Xi(1530)^- \bar{\Xi}^+ + c.c.$ and $J/\psi \to \Xi(1530)^0 \bar{\Xi}^0 + c.c.$. For the $\psi(3686) \to \Xi^- \bar{\Xi}^+$ decay, dominant backgrounds come from $\psi(3686) \to \gamma\chi_{cJ}$, $\chi_{cJ} \to \Xi^- \bar{\Xi}^+$, and $\psi(3686) \to \Sigma(1385)^- \bar{\Sigma}(1385)^+$, which are expected to populate smoothly in the $M_{\pi^-\Lambda}^{\rm recoil}$ spectrum.
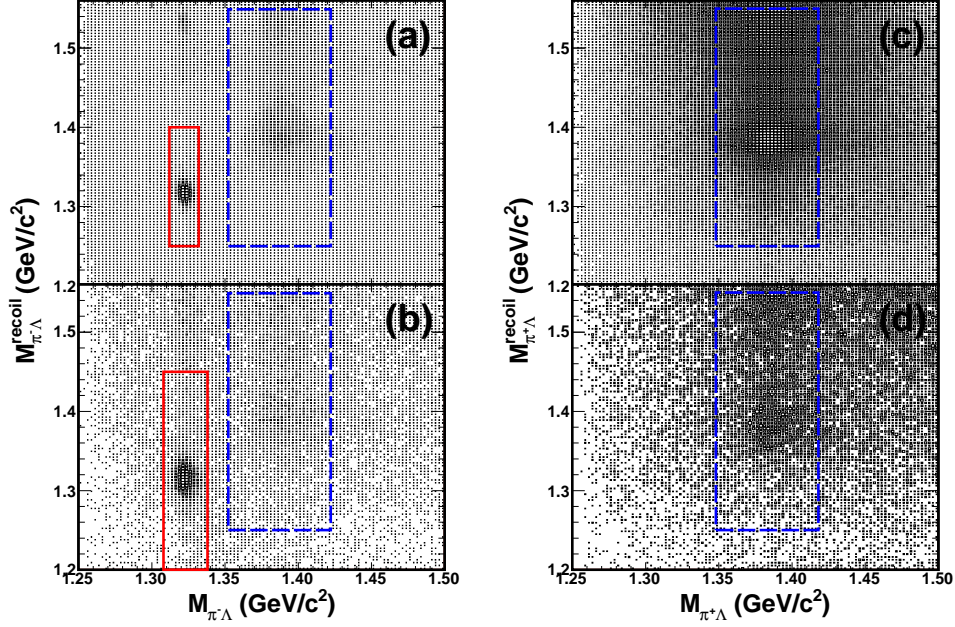
FIG. 1. Scatter plots of $M_{\pi^{\pm}\Lambda}$ versus $M_{\pi^{\pm}\Lambda}^{recoil}$ for (a, c) J/ψ and (b, d) $\psi(3686)$ data. The solid boxes are for the $\Xi^{-}\bar{\Xi}^{+}$ signal region, and the dashed boxes are for the $\Sigma(1385)^{\mp}\bar{\Sigma}(1385)^{\pm}$ signal region.

For the $\psi(3686) \rightarrow \Sigma(1385)^{\mp}\bar{\Sigma}(1385)^{\pm}$ decay, the surviving backgrounds mainly come from the process $\psi(3686) \rightarrow \pi^{+}\pi^{-}J/\psi$.

V. RESULTS

A. Branching fraction

The signal yields for $\psi \rightarrow \Xi^{-}\bar{\Xi}^{+}$, $\Sigma(1385)^{\mp}\bar{\Sigma}(1385)^{\pm}$ are determined by performing an extended maximum likelihood fit to $M_{\pi^{\mp}\Lambda}^{\mathrm{recoil}}$ spectrum. In the fit, the signal shape is represented by a simulated MC shape convoluted with a Gaussian function taking into account the mass resolution difference between data and MC. The background shapes for $\psi \rightarrow \Xi^{-}\bar{\Xi}^{+}$ and $\psi(3686) \rightarrow \Sigma(1385)^{\mp}\bar{\Sigma}(1385)^{\pm}$ are represented by a second-order polynomial function since the peaking backgrounds are found to be negligible and the remaining backgrounds are expected to be distributed smoothly in $M_{\pi^{\mp}\Lambda}^{\mathrm{recoil}}$. In the decay $J/\psi \rightarrow \Sigma(1385)^{\mp}\bar{\Sigma}(1385)^{\pm}$, the peaking background is found to be significant and is included in the fit. The shapes of the peaking backgrounds are represented by the individual shapes taken from simulation, and the corresponding number of background events is fixed accordingly. The remaining backgrounds are described by a second-order polynomial function. Figure 2 shows the projection plots of $M_{\pi^{\mp}\Lambda}^{\mathrm{recoil}}$ for $\psi \rightarrow \Xi^{-}\bar{\Xi}^{+}$ and $\Sigma(1385)^{\mp}\bar{\Sigma}(1385)^{\pm}$.

The branching fractions are calculated by

$$\mathcal{B}[\psi \rightarrow X] = \frac{N_{\mathrm{obs.}}}{N_{\psi} \cdot \epsilon}, \tag{4}$$

where X stands for the $\Xi^{-}\bar{\Xi}^{+}$ and $\Sigma(1385)^{\mp}\bar{\Sigma}(1385)^{\pm}$ final states, ϵ denotes the detection efficiencies taking into account the product branching fraction of the tag mode of $\Xi^{-}(\Sigma(1385)^{\mp})$ decay and the values of α measured in this analysis, $N_{\mathrm{obs.}}$ is the number of signal events from the fit, and N_{ψ} is the total number of J/ψ or $\psi(3686)$ events [17, 18]. Table I summarizes the number of observed signal events, the corresponding efficiencies, and branching fractions for the various decays of this measurement with the statistic uncertainty only.

B. Angular distribution

The values of α for the six decay processes are extracted by performing a least-squares fit to the $\cos\theta$ distributions in the range of 0.8 to -0.8. The $\cos\theta$ distributions are divided into 8 equidistant intervals for the process $\psi(3686) \rightarrow \Sigma(1385)^{\mp}\bar{\Sigma}(1385)^{\pm}$ and into 16 intervals for the other four decay modes.

The signal yield in each $\cos\theta$ bin is obtained with the aforementioned fit method. The distributions of the efficiency-corrected signal yields together with the curves of the fit are shown in Fig. 3. The α values obtained from the fits based on Eq. (2) are summarized in Table I.
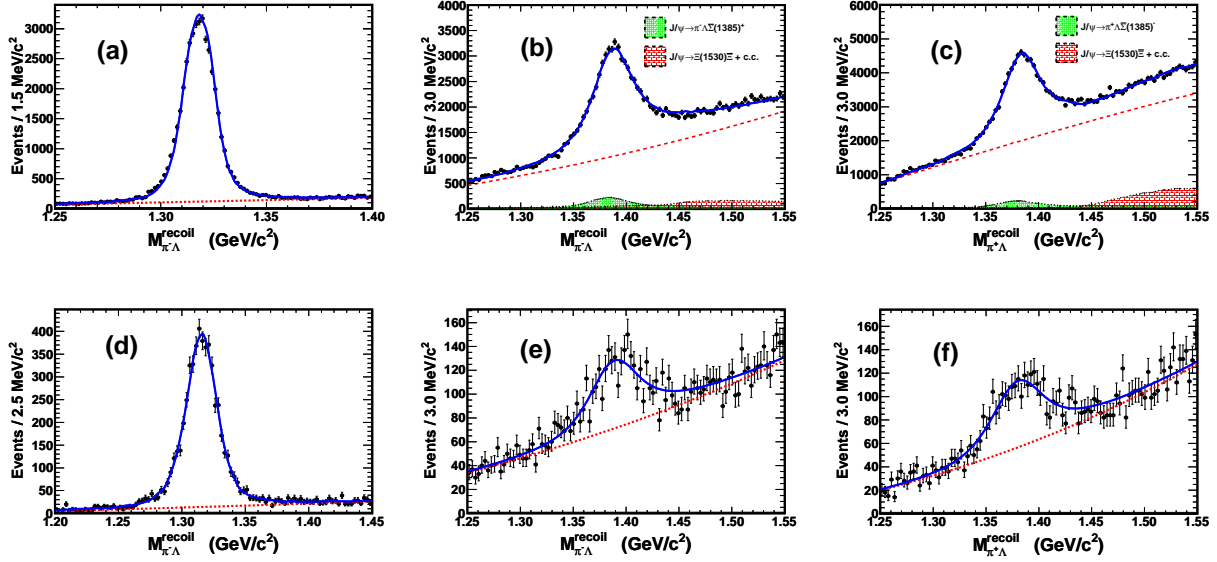
FIG. 2. Recoil mass spectra of $\pi^-\Lambda$ and $\pi^+\Lambda$. (a) $J/\psi \to \Xi^-\bar{\Xi}^+$, (b) $J/\psi \to \Sigma(1385)^-\bar{\Sigma}(1385)^+$, (c) $J/\psi \to \Sigma(1385)^+\bar{\Sigma}(1385)^-$, (d) $\psi(3686) \to \Xi^-\bar{\Xi}^+$, (e) $\psi(3686) \to \Sigma(1385)^-\bar{\Sigma}(1385)^+$ and (f) $\psi(3686) \to \Sigma(1385)^+\bar{\Sigma}(1385)^-$. Dots with error bars indicate the data, the solid lines show the fit results, the dashed lines are for the combinatorial background, and the hatched histograms are for the peaking backgrounds.

TABLE I. The number of the observed events $N_{\mathrm{obs.}}$, efficiencies ϵ, α values, and branching fractions $\mathcal{B}$ for $\psi \to \Xi^-\bar{\Xi}^+$, $\Sigma(1385)^{\mp}\bar{\Sigma}(1385)^{\pm}$. Only statistical uncertainties are indicated.

Channel	$N_{\mathrm{obs.}}$	$\epsilon(\%)$	α	$\mathcal{B}(\times 10^{-4})$
$J/\psi \to \Xi^-\bar{\Xi}^+$	42810.7 ± 231.0	18.40 ± 0.04	0.58 ± 0.04	10.40 ± 0.06
$J/\psi \to \Sigma(1385)^-\bar{\Sigma}(1385)^+$	42594.8 ± 466.8	17.38 ± 0.04	-0.58 ± 0.05	10.96 ± 0.12
$J/\psi \to \Sigma(1385)^+\bar{\Sigma}(1385)^-$	52522.5 ± 595.9	18.67 ± 0.04	-0.49 ± 0.06	12.58 ± 0.14
$\psi(3686) \to \Xi^-\bar{\Xi}^+$	5336.7 ± 82.6	18.04 ± 0.04	0.91 ± 0.13	2.78 ± 0.05
$\psi(3686) \to \Sigma(1385)^-\bar{\Sigma}(1385)^+$	1374.5 ± 97.8	15.12 ± 0.04	0.64 ± 0.40	0.85 ± 0.06
$\psi(3686) \to \Sigma(1385)^+\bar{\Sigma}(1385)^-$	1469.9 ± 94.6	16.45 ± 0.04	0.35 ± 0.37	0.84 ± 0.05

VI. SYSTEMATIC UNCERTAINTY

A. Branching fraction

Systematic uncertainties on the branching fractions are mainly due to efficiency and resolution differences between data and MC. They are estimated by comparing the efficiencies of tracking, PID, Λ and Ξ^- reconstruction, and the $\pi^{\mp}\Lambda$ mass window requirement of the reconstructed $\Xi(\Sigma(1385)^{\mp})$ between the data and simulation. Additional sources of systematic uncertainties are the fit range, the background shape, the angular distributions, and the mass shift in $M_{\pi^{\mp}\Lambda}^{recoil}$. In addition, the uncertainties of the decay branching fractions of intermediate states and uncertainties of the total number of ψ events are also accounted for in the systematic uncertainty. All of the systematic uncertainties are discussed in detail below.

1. The uncertainties due to the tracking and PID efficiencies of the π originating from $\Sigma(1385)$ decays are in-vestigated with the control sample $J/\psi \to p\bar{p}\pi^+\pi^-$. It is found that the efficiency difference between data and MC is 1.0% per pion for track reconstruction and PID, respectively, taking into account the relative low momentum. These differences are taken as systematic uncertainties.

2. The uncertainty of the Λ reconstruction efficiency in $\Sigma(1385)$ decays is estimated using the control sample $\psi \to \Xi^-\bar{\Xi}^+$. A detailed description of this method can be found in [25]. The differences of Λ reconstruction efficiency between data and MC are found to be 3.0% and 1.0% in the J/ψ and $\psi(3686)$ decay respectively, which are taken into account as systematic uncertainties.

3. The Ξ reconstruction efficiency, which includes the tracking and PID efficiencies for the pion from the Ξ decay and the Λ reconstruction efficiency, is studied with the control samples $\psi \to \Xi^-\bar{\Xi}^+$ reconstructed via sin-
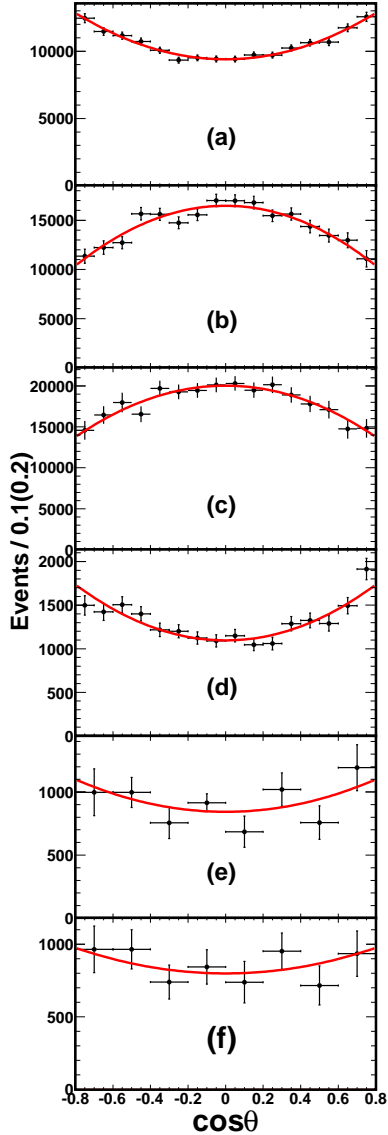
FIG. 3. Distributions of $\cos\theta$ for the signals of (a) $J/\psi \to \Xi^-\bar{\Xi}^+$, (b) $J/\psi \to \Sigma(1385)^-\bar{\Sigma}(1385)^+$, (c) $J/\psi \to \Sigma(1385)^+\bar{\Sigma}(1385)^-$, (d) $\psi(3686) \to \Xi^-\bar{\Xi}^+$, (e) $\psi(3686) \to \Sigma(1385)^-\bar{\Sigma}(1385)^+$ and (f) $\psi(3686) \to \Sigma(1385)^+\bar{\Sigma}(1385)^-$. The dots with error bars indicate the efficiency-corrected signal yields in data, and the curves show the fit results.

gle and double tag methods. The selection criteria of the charged tracks, and the reconstruction of Λ and Ξ candidates are exactly the same as those described in Sec. III. The Ξ^- reconstruction efficiency is defined as the ratio of the number of events from the double tag $\Xi^-\bar{\Xi}^+$ to that from the single tag. The difference in the Ξ reconstruction efficiency between data and MC samples is taken as the systematic uncertainty.

4. For $\psi \to \Sigma(1385)^-\bar{\Sigma}(1385)^+$, a strict requirement for the mass window of $\pi^\mp\Lambda$ with $1\,\sigma$ level is applied to suppress backgrounds, where the width σ of the charged $\Sigma(1385)$ mass is $35 \sim 40$ MeV [3]. We vary the nominal requirements by ± 10 MeV/c^2 and take the difference between the data and the MC as the systematic uncertainty due to mass window of $\pi^\mp\Lambda$. For the Ξ channels, the systematic uncertainty due to mass window of $\pi^\mp\Lambda$ is estimated to be negligible.

5. In the fits of the $M^{\rm recoil}_{\pi^\mp\Lambda}$ spectrum, the uncertainty due to the fit range is estimated by changing the fit range by ± 10 MeV/c^2. The differences of the signal yields are taken as the systematic uncertainties.

6. The uncertainty related to the shape of nonpeaking backgrounds, which is described by a second-order polynomial function in the fit, is estimated by repeating the fit with a first or a third-order polynomial. The largest difference in the signal yield with respect to the nominal yields is taken as the systematic uncertainty. In the decay $J/\psi \to \Sigma(1385)^\mp\bar{\Sigma}(1385)^\pm$, the uncertainty related to the peaking background is estimated by varying the normalized number of background events by 1σ. The signal yield changes are taken as the systematic uncertainty related to the peaking background. The total uncertainty related to the background are obtained by adding the individual contributions in quadrature.

7. The uncertainty in the detection efficiency due to the modeling of the angular distribution of the baryon pairs, represented by the parameter α, is estimated by varying the measured α values by 1σ. The relative change in the detection efficiency is taken as a systematic uncertainty.

8. Due to the imperfection of the simulation of the momentum spectrum of the pion from Ξ or $\Sigma(1385)$ decays, a mass shift (~ 2 MeV/c^2) between data and MC is observed in the $M^{\rm recoil}_{\pi^\mp\Lambda}$ spectrum for the J/ψ decays (the mass shift in $\psi(3686)$ decay is negligible), which may affect the signal yields since they are obtained by fitting with the corresponding MC shape convoluted with a Gaussian function. To estimate the corresponding effect, the shift of the $M^{\rm recoil}_{\pi^\mp\Lambda}$ spectrum for the simulated exclusive MC events is corrected, and then the data are refitted with the same method as the nominal fit. The resulting changes in signal yields are taken as the systematic uncertainty.

9. The uncertainties in the branching fractions of the decays of the intermediate states, Ξ, $\Sigma(1385)$ and Λ, are taken from PDG [3] (0.8% for $\psi \to \Xi^-\bar{\Xi}^+$ and 1.9% for $\psi \to \Sigma(1385)^\mp\bar{\Sigma}(1385)^\pm$); they are considered as systematic uncertainties.

10. The systematic uncertainties due to the total number of J/ψ or $\psi(3686)$ events are determined with inclusive hadronic ψ decays; they are 0.6% and 0.8% for J/ψ and $\psi(3686)$ [17, 18], respectively.

The various contributions of the systematic uncertainties on the branching fraction measurements are summarized in Table II. The total systematic uncertainty is obtained by summing the individual contributions in quadrature.

B. Angular distribution

Various systematic uncertainties are considered in the measurement of α values. These include the uncertainty of the signal yield in the different $\cos\theta$ intervals, the uncertainty of $\cos\theta$ fit procedure, and the uncertainty related to the detection efficiency correction curve as function of $\cos\theta$ bin. They are summarized in Table III and are discussed in detail below.

1. The signal yields in each $\cos\theta$ interval are extracted from the fit to the corresponding $M_{\pi\mp\Lambda}^{recoil}$ distribution. The sources of the systematic uncertainty of the signal yield include the fit range, the background shape, and the mass shift in the $M_{\pi\mp\Lambda}^{recoil}$ distribution. To estimate the systematic uncertainty related to the fit range on $M_{\pi\mp\Lambda}^{recoil}$, we repeat the fit to the $M_{\pi\mp\Lambda}^{recoil}$ by changing the fit range by $\pm$ 10 MeV/c^2. Then, the α values are extracted by the fit with the changed signal yields, and the resulting differences to the nominal α values are taken as the systematic uncertainties. Analogously, the uncertainties related to the background shape and the mass shift in $M_{\pi\mp\Lambda}^{recoil}$ distribution are evaluated with the method described above.

2. The systematic uncertainties related to the fit procedure of the $\cos\theta$ distributions are estimated by refitting the $\cos\theta$ distribution with a different binning and fit range. We divide $\cos\theta$ into 8 intervals for $\psi \rightarrow \Xi^-\bar{\Xi}^+$, $J/\psi \rightarrow \Sigma(1385)^\mp\bar{\Sigma}(1385)^\pm$ and 16 intervals for $\psi(3686) \rightarrow \Sigma(1385)^\mp\bar{\Sigma}(1385)^\pm$. The changes of the α values are taken as systematic uncertainties. We also repeat the fit by changing the range to $[-0.9, 0.9]$ and $[-0.7, 0.7]$ in $\cos\theta$, with the same bin size and different number of bins as the nominal fit. The largest difference in α with respect to the nominal value is taken as the systematic uncertainty.

3. In the analysis, the α values are obtained by fitting the $\cos\theta$ distribution corrected for the detection efficiency. To estimate the systematic uncertainty related to the imperfection of simulation of detection efficiency, the ratio of detection efficiencies between data and MC simulation is obtained based on the control sample $J/\psi \rightarrow \Xi^-\bar{\Xi}^+$ with a full event reconstruction. Then, the $\cos\theta$ distribution corrected by the ratio of detection efficiencies is refitted. The resulting differences in α are taken as the systematic uncertainty.

All the systematic uncertainties for the α measurement are summarized in Table III. The total systematic uncertainty is the quadratic sum of the individual uncertainties, assuming them to be independent.

VII. CONCLUSION AND DISCUSSION

Using $(225.3 \pm 2.8) \times 10^6$ J/ψ and $(106.4 \pm 0.9) \times 10^6$ $\psi(3686)$ events collected with the BESIII detector at BEPCII, the branching fractions and the angular distributions for $\psi \rightarrow \Xi^-\bar{\Xi}^+$ and $\Sigma(1385)^\mp\bar{\Sigma}(1385)^\pm$ are measured. A comparison of the branching fractions and α values between our measurements and previous experiments is summarized in Tables IV and V, where the branching fractions for $\psi(3686) \rightarrow \Sigma(1385)^\mp\bar{\Sigma}(1385)^\pm$ and the angular distributions for $\psi(3686) \rightarrow \Xi^-\bar{\Xi}^+$ and $\Sigma(1385)^\mp\bar{\Sigma}(1385)^\pm$ are measured for the first time. The branching fractions and angular distributions for $J/\psi \rightarrow \Xi^-\bar{\Xi}^+$, $\Sigma(1385)^\mp\bar{\Sigma}(1385)^\pm$ and the branching fraction for $\psi(3686) \rightarrow \Xi^-\bar{\Xi}^+$ are in good agreement and much more precise compared to previously published results. The measured α values are also compared with the predictions in theoretical models [10, 11]. As indicated in Table V, most of our results disagree significantly with the theoretical predictions, which implies that the naive prediction of QCD suffers from the approximation that higher-order corrections are not taken into account. The theoretical models are expected to be improved in order to understand the origin of these discrepancies.

To test the "12% rule," the branching fraction ratios $\frac{\mathcal{B}(\psi(3686)\rightarrow\Xi^-\bar{\Xi}^+)}{\mathcal{B}(J/\psi\rightarrow\Xi^-\bar{\Xi}^+)}$, $\frac{\mathcal{B}(\psi(3686)\rightarrow\Sigma(1385)^-\bar{\Sigma}(1385)^+)}{\mathcal{B}(J/\psi\rightarrow\Sigma(1385)^-\bar{\Sigma}(1385)^+)}$ and $\frac{\mathcal{B}(\psi(3686)\rightarrow\Sigma(1385)^+\bar{\Sigma}(1385)^-)}{\mathcal{B}(J/\psi\rightarrow\Sigma(1385)^+\bar{\Sigma}(1385)^-)}$ are calculated to be $(26.73 \pm 0.50 \pm 2.30)\%$, $(7.76 \pm 0.55 \pm 0.68)\%$ and $(6.68 \pm 0.40 \pm 0.50)\%$, respectively, taking into account common systematic uncertainties. The ratios are not in agreement with 12%, especially for the $\Xi^-\bar{\Xi}^+$ mode.

TABLE II. Systematic uncertainties on the branching fraction measurements (%).

Source	$J/\psi \to$			$\psi(3686) \to$		
Mode	$\Xi^-\bar\Xi^+$	$\Sigma(1385)^-\bar\Sigma(1385)^+$	$\Sigma(1385)^+\bar\Sigma(1385)^-$	$\Xi^-\bar\Xi^+$	$\Sigma(1385)^-\bar\Sigma(1385)^+$	$\Sigma(1385)^+\bar\Sigma(1385)^-$
MDC tracking	—	1.0	1.0	—	1.0	1.0
PID	—	1.0	1.0	—	1.0	1.0
Λ reconstruction	—	3.0	3.0	—	1.0	1.0
Ξ reconstruction	6.6	—	—	4.4	—	–
Mass window of $\pi\Lambda$	negligible	2.1	1.1	negligible	2.4	2.4
Fit range	0.2	2.3	1.5	0.2	3.5	1.5
Background shape	1.0	3.6	4.2	1.5	4.5	4.0
Angular distribution	1.0	2.0	1.5	1.2	3.0	2.6
Mass shift in $M^{recoil}_{\pi^\mp\Lambda}$	2.0	1.0	0.5	negligible	negligible	negligible
Branching fraction	0.8	1.9	1.9	0.8	1.9	1.9
Total number of ψ	0.6	0.6	0.6	0.8	0.8	0.8
Total	7.1	6.5	6.2	4.9	7.4	6.2

TABLE III. Systematic uncertainties on α value measurements (%).

Source	$J/\psi \to$			$\psi(3686) \to$		
Mode	$\Xi^-\bar\Xi^+$	$\Sigma(1385)^-\bar\Sigma(1385)^+$	$\Sigma(1385)^+\bar\Sigma(1385)^-$	$\Xi^-\bar\Xi^+$	$\Sigma(1385)^-\bar\Sigma(1385)^+$	$\Sigma(1385)^+\bar\Sigma(1385)^-$
$M^{recoil}_{\pi^\mp\Lambda}$ fitting range	6.6	5.2	7.3	9.1	7.8	6.2
Background shape	5.7	5.2	5.9	7.7	28.0	11.0
Mass shift in $M^{recoil}_{\pi^\mp\Lambda}$	4.5	5.8	6.0	negligible	negligible	negligible
$\cos\theta$ interval	1.5	2.0	4.0	5.6	16.0	15.0
$\cos\theta$ fit range	5.3	10.5	8.2	6.6	25.0	20.0
Efficiency correction	6.9	5.1	5.5	5.4	6.1	6.7
Total	13.2	15.1	15.4	15.7	42.0	28.8

TABLE IV. Comparison of the branching fractions for $\psi \to \Xi^-\bar\Xi^+$, $\Sigma(1385)^\mp\bar\Sigma(1385)^\pm$ (in units of 10^{-4}). The first uncertainties are statistical, and the seconds are systematic.

Source	$J/\psi \to$			$\psi(3686) \to$		
Mode	$\Xi^-\bar\Xi^+$	$\Sigma(1385)^-\bar\Sigma(1385)^+$	$\Sigma(1385)^+\bar\Sigma(1385)^-$	$\Xi^-\bar\Xi^+$	$\Sigma(1385)^-\bar\Sigma(1385)^+$	$\Sigma(1385)^+\bar\Sigma(1385)^-$
This work	$10.40 \pm 0.06 \pm 0.74$	$10.96 \pm 0.12 \pm 0.71$	$12.58 \pm 0.14 \pm 0.78$	$2.78 \pm 0.05 \pm 0.14$	$0.85 \pm 0.06 \pm 0.06$	$0.84 \pm 0.05 \pm 0.05$
MarkI [5]	14.00 ± 5.00	—	—	< 2.0	—	—
MarkII [6]	$11.40 \pm 0.80 \pm 2.00$	$8.60 \pm 1.80 \pm 2.20$	$10.3 \pm 2.4 \pm 2.5$	—	—	—
DM2 [7]	$7.00 \pm 0.60 \pm 1.20$	$10.00 \pm 0.40 \pm 2.10$	$11.9 \pm 0.4 \pm 2.5$	—	—	—
BESII [8, 12]	$9.00 \pm 0.30 \pm 1.80$	$12.30 \pm 0.70 \pm 3.00$	$15.0 \pm 0.8 \pm 3.8$	$3.03 \pm 0.40 \pm 0.32$	—	—
CLEO [9]	—	—	—	$2.40 \pm 0.30 \pm 0.20$	—	—
BESI [26]	—	—	—	$0.94 \pm 0.27 \pm 0.15$	—	—
PDG [3]	8.50 ± 1.60	10.30 ± 1.30	10.30 ± 1.30	1.80 ± 0.60	—	—

TABLE V. Comparison of α for $\psi \to \Xi^-\bar\Xi^+$ and $\Sigma(1385)^\mp\bar\Sigma(1385)^\pm$. The first uncertainties are statistical, and the second are systematic.

Source	$J/\psi \to$			$\psi(3686) \to$		
Mode	$\Xi^-\bar\Xi^+$	$\Sigma(1385)^-\bar\Sigma(1385)^+$	$\Sigma(1385)^+\bar\Sigma(1385)^-$	$\Xi^-\bar\Xi^+$	$\Sigma(1385)^-\bar\Sigma(1385)^+$	$\Sigma(1385)^+\bar\Sigma(1385)^-$
This work	$0.58 \pm 0.04 \pm 0.08$	$-0.58 \pm 0.05 \pm 0.09$	$-0.49 \pm 0.06 \pm 0.08$	$0.91 \pm 0.13 \pm 0.14$	$0.64 \pm 0.40 \pm 0.27$	$0.35 \pm 0.37 \pm 0.10$
BESII [8]	$0.35 \pm 0.29 \pm 0.06$	$-0.54 \pm 0.22 \pm 0.10$	$-0.35 \pm 0.25 \pm 0.06$	—	—	—
MarkIII [6]	0.13 ± 0.55	—	—	—	—	—
Claudson et al. [10]	0.16	0.11	0.11	0.32	0.29	0.29
Carimalo [11]	0.27	0.20	0.20	0.52	0.50	0.50

[1] J. Bolz and P. Kroll, Eur. Phys. J. C **2**, 545 (1998); S. J. Brodsky and G. P. Lepage, Phys. Rev. D **24**, 2848 (1981).

[2] T. Appelquist and H. D. Politzer, Phys. Rev. Lett. **34**, 43 (1975); A. De Rujula and S. L. Glashow, Phys. Rev. Lett. **34**, 46 (1975); W. S. Hou and A. Soni, Phys. Rev. Lett. **50**, 569 (1983); W. S. Hou, Phys. Rev. D **55**, 6952 (1997).

[3] K. A. Olive *et al.* (Particle Data Group), Chin. Phys. C **38**, 090001 (2014).

[4] Y. F. Gu and X. H. Li, Phys. Rev. D **63**, 114019 (2001); X. H. Mo, C. Z. Yuan and P. Wang, High Energy Physics and Nuclear Physics **31**, 686 (2007); N. Brambilla *et al.* (Quarkonium Working Group), Eur. Phys. J. C **71**, 1534 (2011); Q. Wang, G. Li, and Q. Zhao, Phys. Rev. D **85**, 074015 (2012).

[5] I. Peruzzi, M. Piccolo, M. S. Alam, A. Boyarski, M. Breidenbach, G. J. Feldman, G. Hanson and J. Jaros *et al.*, Phys. Rev. D **17**, 2901 (1978).

[6] M. W. Eaton, G. Goldhaber, G. S. Abrams, C. A. Blocker, W. C. Carithers, W. Chinowsky, M. W. Coles and S. Cooper *et al.*, Phys. Rev. D **29**, 804 (1984).

[7] P. Henrard *et al.* (DM2 Collaboration), Nucl. Phys. **B292**, 670 (1987).

[8] M. Ablikim *et al.* (BESII Collaboration), Chin. Phys. C **36**, 1031 (2012).

[9] T. K. Pedlar *et al.* (CLEO Collaboration), Phys. Rev. D **72**, 051108 (2005).

[10] M. Claudson, S. L. Glashow and M. B. Wise, Phys. Rev. D **25**, 1345 (1982).

[11] C. Carimalo, Int. J. Mod. Phys. A **2**, 249 (1987).

[12] M. Ablikim *et al.* (BES Collaboration), Phys. Lett. B **648**, 149 (2007).

[13] J. Z. Bai *et al.* (BES Collaboration), Phys. Lett. B **591**, 42 (2004).

[14] M. Ablikim *et al.* (BES Collaboration), Phys. Lett. B **632**, 181 (2006).

[15] M. Ablikim *et al.* (BESIII Collaboration), Study of $\psi \to \Lambda\bar{\Lambda}$ and $\Sigma^0\bar{\Sigma}^0$ decays, to be published.

[16] M. Ablikim *et al.* (BESIII Collaboration), Chin. Phys. C **36**, 915 (2012).

[17] With the same method (see Ref. [16] for more details), the preliminary number of the updated J/ψ events taken in 2009 determined to be 223.7×10^6 with an uncertainty of 0.6%.

[18] M. Ablikim *et al.* (BESIII Collaboration), Chin. Phys. C **37**, 063001 (2013).

[19] M. Ablikim *et al.* (BESIII Collaboration), Nucl. Instrum. Methods Phys. Res., Sect A **614**, 345 (2010).

[20] S. Agostinelli *et al.* (GEANT4 Collaboration), Nucl. Instrum. Methods Phys. Res., Sect A **506**, 250 (2003).

[21] J. Allison *et al.*, IEEE Trans. Nucl. Sci. **53**, 270 (2006).

[22] S. Jadach, B. F. L. Ward and Z. Was, Comput. Phys. Commun. **130**, 260 (2000); S. Jadach, B. F. L. Ward and Z. Was, Phys. Rev. D **63**, 113009 (2001).

[23] D. J. Lange, Nucl. Instrum. Methods Phys. Res., Sect A **462**, 152 (2001); R. G. Ping, Chin. Phys. C **32**, 599 (2008).

[24] J. C. Chen, G. S. Huang, X. R. Qi, D. H. Zhang and Y. S. Zhu, Phys. Rev. D **62**, 034003 (2000).

[25] M. Ablikim *et al.* (BESIII Collaboration), Phys. Rev. D **87**, no. 3, 032007 (2013) [Phys. Rev. D **87**, no. 5, 059901 (2013)].

[26] J. Z. Bai *et al.* (BES Collaboration), Phys. Rev. D **63**, 032002 (2001).